Chapter 2

Experimental Techniques

Contents

2. Experimental Techniques
   - 2.1 Introduction 36
   - 2.2 Mossbauer Spectroscopy 36
     - 2.2.1 Mossbauer source and absorber 38
     - 2.2.2 Drive unit 40
     - 2.2.3 Gamma ray detector and data acquisition system 40
     - 2.2.4 Data Analysis 41
     - 2.2.5 Velocity Calibration 43
   - 2.3 Time Differential Perturbed Angular Correlation technique 43
     - 2.3.1 Experimental Setup 43
     - 2.3.2 Data Reduction and Error Analysis 46
     - 2.3.3 Time Calibration of TDPAC spectrometer 47
   - 2.4 AC Susceptibility 48
     - 2.4.1 Introduction 48
     - 2.4.2 Basic Principles 49
   - 2.5 Hall Effect 51
     - 2.5.1 Introduction 51
     - 2.5.2 Importance of hall effect 52
     - 2.5.3 Magnetoresistance 53
   - References 54

Experimental Techniques

2.1 Introduction

This chapter discusses about the experimental techniques used in the study of magnetic materials presented in this thesis. Basic techniques like Mossbauer Spectroscopy and Time Differential Perturbed Angular Correlations (TDPAC) were employed for studying the hyperfine interactions in the materials. The important feature of these techniques is that, they are sensitive to very low probe concentration (~ 10^{13}- 10^{17} atoms/cm3). The other techniques used were AC Susceptibility (to study the phenomena of Magnetism) and Hall Effect (to determine the charge carrier density and transport properties).

2.2 Mossbauer Spectroscopy

Mossbauer Spectra are usually recorded in transmission geometry using a constant acceleration spectrometer operated in conjunction with a multi channel analyzer in the Multi Scaling Mode(MCS). In this geometry the source is vibrated whose velocity is linearly increased and decreased in successive half periods of oscillation to Doppler modulate the gamma energy. The source velocity is adjusted in such a way that full spectrum can be recorded. For this purpose multichannel acquisition system is used, the a switching of registered channel occurs synchronically with linearly changing speed of the source.

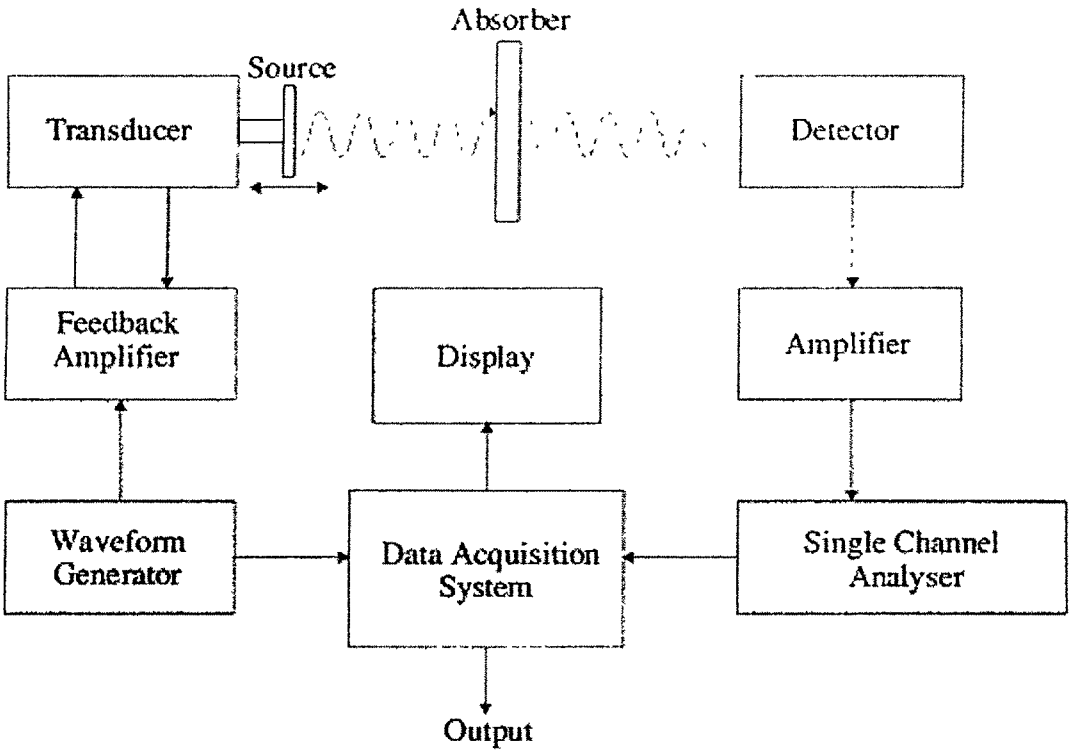

Fig 2.1 Block Diagram Mossbauer Spectrometer

As shown in the Fig 2.1 Mössbauer setup consists of basically

1. Mossbauer source and absorber
2. Drive unit
3. Gamma ray detector
4. Data acquisition system

2.2.1. Mössbauer Source and Absorber :

a. Source

The source used in the study of Mössbauer spectroscopy was ^{57}Co. This was embedded in a rhodium matrix which provides a solid environment for the ^{57}Co atoms with a high recoil free fraction and a cubic, non magnetic site environment to produce mono energetic gamma rays (Single Line Spectrum)

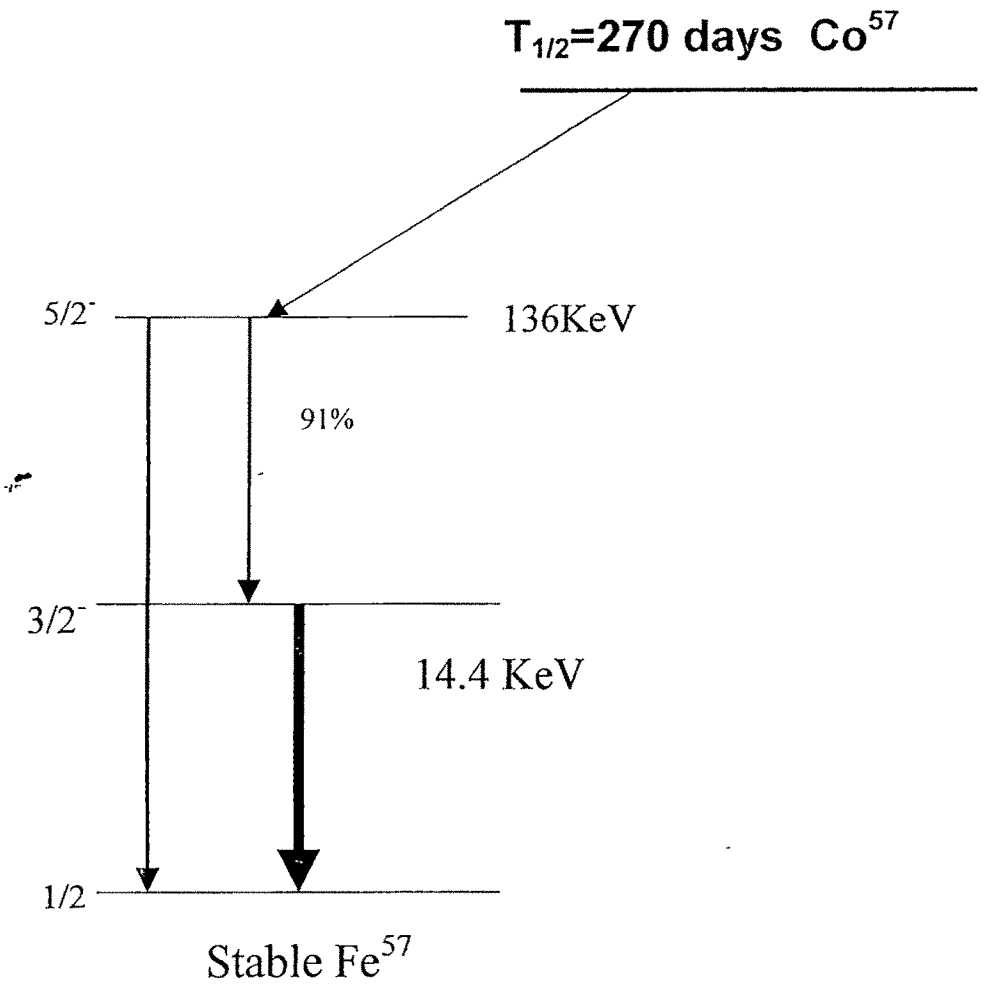

Fig 2.2 Decay Scheme of Co^{57} source

The decay scheme of this isotope is shown in Fig 2.2. The half life of ^{57}Co is 271.7 days and decays via electron capture to I=5/2 excited state of ^{57}Fe. 91% of this excited state decays to I=3/2 first excited state (14.4 KeV) and the remaining 9% to the I=1/2 ground state by gamma ray emission. The 14.4 KeV state in turn decays to ground state by gamma ray emission or internal conversion. The mean life time of this I=3/2 state is 97.8 ns which corresponds to the natural line width of 0.194 mm/sec.

b. Absorber

Mossbauer absorbers used in the present study were antimony based dilute alloys. The separated 95% enriched ^{57}Fe isotope was used in making such dilute alloys. As such natural abundance of ^{57}Fe in iron powder is just 2% (i.e. 2×10^{13} ^{57}Fe nuclei/cm^2). So if the samples are made with Fe in very dilute quantity, then one needs to use enriched isotope ^{57}Fe instead of natural Fe so that proper statistics of the data can be obtained. Hence ^{57}Fe enriched isotope was used for making our samples. The samples for Mossbauer absorber were finely powdered by grinding them using a mortar and pestle. Approximately 100 mg of the sample was taken and spread uniformly in a 1.2cm^2 area.

2.2.2 Drive Unit

Drive unit consists of a velocity transducer, on the axle of which the source is mounted and is driven by the magnetic force produced by a drive current in the coil. The resulting motion induces a current in a sensing coil that is proportional to the velocity. This sensed current is compared to a reference current ramp, and the difference (error) signal is feedback to the drive current amplifier in such a manner as to reduce the difference between the sensed current and the reference current , keeping the velocity of the axle precisely proportional to the reference current.

The reference current is a sawtooth function or triangular function of a time with a slow linear rise from $-I_0$ to $+I_0$ with a rapid flyback to $-I_0$. The corresponding velocity of the axle is therefore also a sawtooth or triangular function of time from $-V_0$ to V_0. The maximum velocity imparted to the source is ±25mm/sec. The synchronous signal (MSB signal) of the MCS is used to trigger an independent ramp generator in the velocity drive circuit.

2.2.3 Gamma ray detector and Data Acquisition system.

The detector used is a proportional counter containing a 90% Krypton and 10% methane gas mixture. The applied bias voltage was around 2KV. The pulse magnitude from the detector is directly proportional to the gamma ray energy. This out put pulse from the counter is amplified and differentiated by the

preamplifier. Further amplification of the pulse is provided by the main amplifier and its output is supplied to a Single Channel Analyzer (SCA). The SCA is set to discriminate against the non 14.4 KeV signals. The signals accepted by the SCA is given to the input of the MCA. The signals in the form of counts are accumulated in 512 channels for one complete cycle and contains two complete spectra. One for positive acceleration and another for negative acceleration of the source. As the acceleration is constant, the time interval is equal for all velocity intervals hence each channel records for the same amount of time through clock controlled rate. During analysis full spectrum is folded around the center point to produce a single spectrum. This increases the number of counts (gives better statistics) and flattens the background profile produced by the difference in intensity of the source radiation.

2.2.4 Data Analysis

The data from above folded spectra were analysed by using 'Meerwal' lorentzian curve fitting program for evaluating the Hyperfine parameters. The minimum in $\chi 2$ is tested by specifying number of random parameter displacements, after each of which a new fitting cycle is initiated, retaining the optimum parameters.

The computer analysis of Mossbauer data yielded peak position, intensity, linewidth and total area of the spectrum. From these parameters the value of isomer shift, Quadrupole splitting, line width and Magnetic spliting were evaluated using the velocity spectrum.

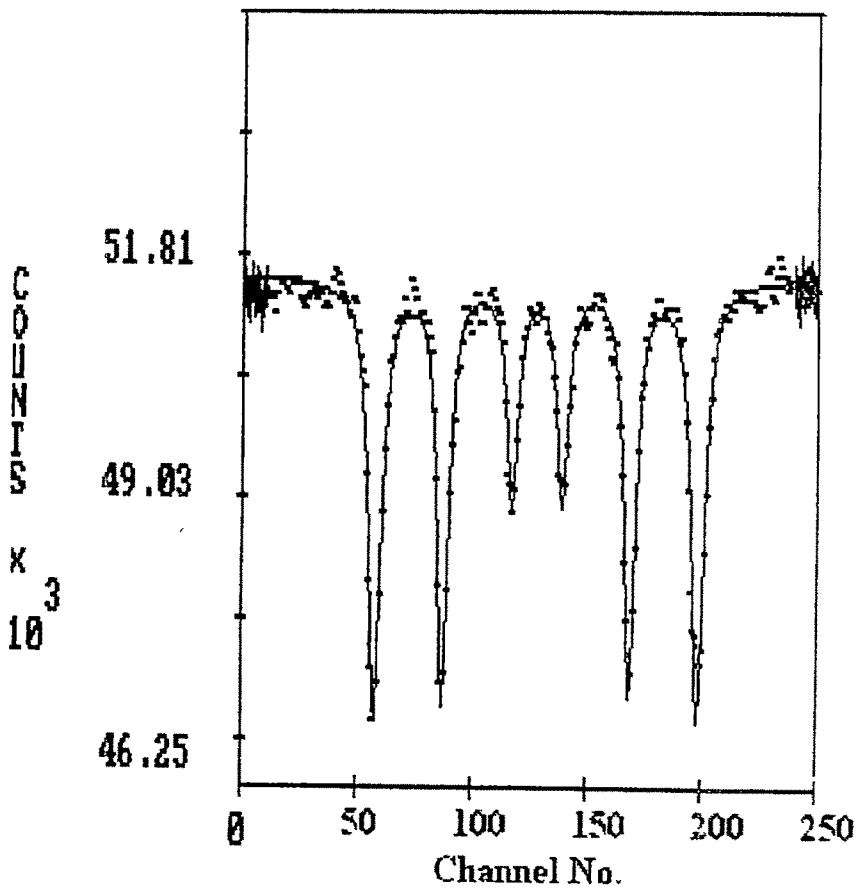

Fig 2.3 Mossbauer spectra of Natural Iron

2.2.5 Velocity Calibration:

The velocity calibration was done using natural Iron as an absorber and Co^{57} as source. It was calculated as 0.028 mm/sec per channel. The resolution of our spectrometer was 0.28 mm/sec. Fig 2.3 shows the calibration spectra of the same.

2.3 Time Differential Perturbed Angular Correlation (TDPAC) Technique

2.3.1 Experimental Setup

Basic spectrometer needs atleast two detectors to measure the angular correlation between γ_1 and γ_2 as a function of time elapsed between the arrival of both photons with in the life time of the intermediate state. Thus the electronic setup has to measure the energy E_γ and arrival time t_γ for each photon. In our setup we have used three BaF_2 (BaF_2 detectors have a very good time resolution and reasonable energy resolution) scintillator detectors for increasing the counting efficiency. Out of three, one detector is used for a start signal and the other two detectors kept at 90 and 180 angles relatively are used for a stop signal. The signals extracted from the PMT tubes attached with detectors are fed to further electronic circuit consisting of *slow-fast coincidence channel*. Fig 2.4 shows the block diagram of TDPAC Setup.

Slow channel mainly consists of Pre Amplifier, linear amplifier, Single Channel analyzer (SCA) and Universal coincidence unit (UC). It is used for processing the

Fig 2.4 Block Diagram of TDPAC setup

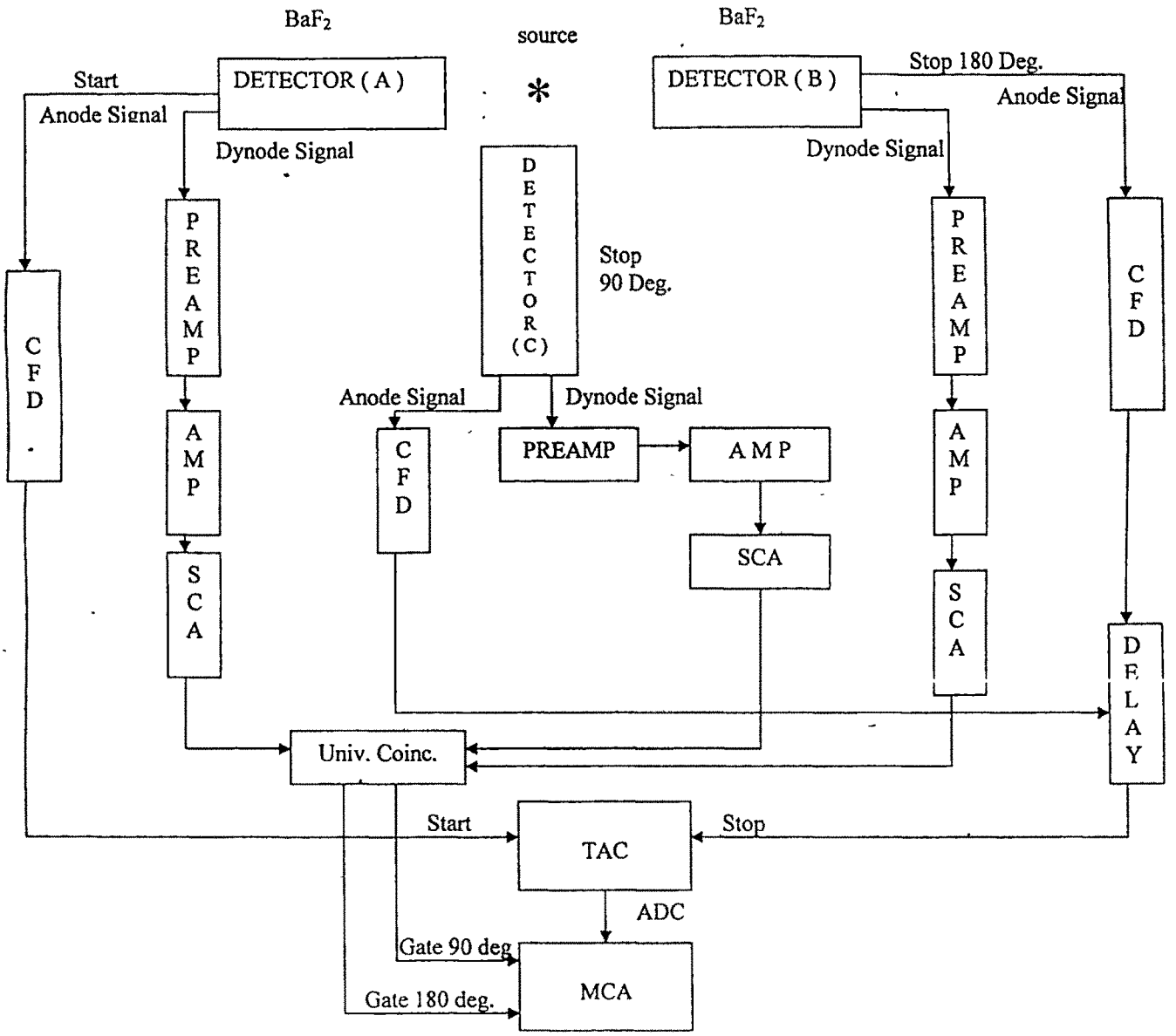

energy pulse having slow rise time. The slow pulse extracted from the 10^{th} dynode of pmt tube is fed to preamplifier for impedance matching. The output of each preamplifier is given to spectroscopic amplifier for Gaussian signal and proper gain. This signal is further fed to SCA, which selects particular gamma rays of start or stop signal by selected window setup. The SCA output from two stop detectors are connected to twin UC unit. And the SCA output from start detector is divided and each is connected to the above mentioned coincidence units. The logical output is produced by the UC when the two signals arrive within this time.

In Fast coincidence channel the main electronic modules involved are Constant fraction discriminator (CFD) and Time to Amplitude Convertor (TAC). The anode pulse from the detector of start channel is fed to CFD unit and the anode pulses from other two detectors of stop channels are first mixed and then given to CFD unit. The negative output from the stop side is further delayed by nano second delay unit and then fed to the TAC input. The time between TAC inputs from Start and Stop signals is converted into voltage pulse by the unit which is positive analog signal. This analog signal is then fed to the input of the MCA.

The two slow coincidence outputs from UC unit will gate the MCA which results in the time spectra of 90^0 and 180^0.

2.3.2 Data Reduction and Error Analysis:

The coincidence rates of the time spectra recorded at 90° and 180° are given by,

$$I_{ij}(\theta,t) = I_0 \varepsilon_i \varepsilon_j e^{-t} / \tau w(\theta,t)$$

The exponential factor describes the decay of the isomer state with mean lifetime τ. I_0 is the rate of decay at t=0. The efficiencies of the detectors are $\varepsilon_i \varepsilon_j$.

The angular correlation function $w(\theta,t)$ is given by,

$$w(\theta,t) = 1 + G_{22}A_{22}P_2(\cos\theta) + G_{44}A_{44}P_4(\cos\theta)$$

while the number of accidental coincidence is given by

$$B_{ij} = 2\tau_0 N_i N_j$$

Where τ_0 is the resolving time, N_i , N_j are the count rates of single events in the respective counters The chance coincidence counts are subtracted from the number of coincidence counts recorded in each channel.

The exponential factor and the detector efficiencies can be eliminated by forming the ratio

$$R(t) = \frac{2[W(180°,t) - W(90°,t)]}{W(180°,t) + 2W(90°,t)},$$

The normalized anisotropy R(t) spectra were least square fitted to a theoretical function of the form

$$R(t) = A_{22}G_{22}(t) = A_{22}\sum_{i=1}^{n} f_i \sum S_{2n} \cos(R\omega(t)) \exp(-R\delta\omega(t)),$$

where, $G_{22}(t)$ is the perturbation factor, ω is the precession frequency related to the quadrupole interaction frequency $\nu_Q = (eQV_{ZZ})/h$ and R is a function of $\eta=(V_{xx}-V_{yy})/V_{zz}$. The V_{xx}, etc. are the EFG components in the principal axis system. $\delta\omega=\delta\nu_Q / \nu_Q$ is the distribution in EFG.

The S_{2n} values determines the orientation of the EFG tensor and also depends on the asymmetry parameter. The spectra were fitted using the program written in FORTRAN language.

2.3.3 Time Calibration of TDPAC Spectrometer

The system was calibrated using Na^{22} source . Prompt spectra of this source was recorded in the MCA. Time range of 500 ns was set in TAC. The Position of prompt peak was noted. The delay between start and stop signals were changed in steps of 8 ns and the corresponding shift in the prompt peak position was recorded. The graph of time delay vs Channel number was plotted. The time calibration was obtained from the slope of the resulting line and it was found to be 0.45 ns/channel.

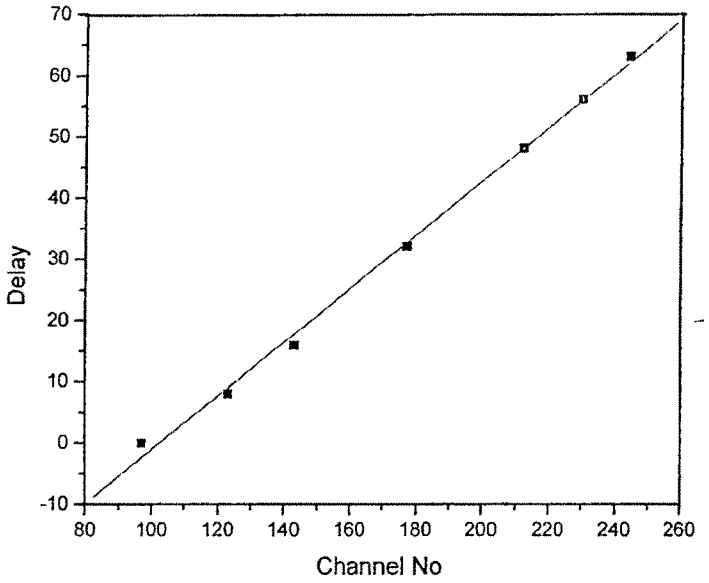

Graph-1

2.4 AC Susceptibility

2.4.1 Introduction:

It is an excellent tool for probing the static and dynamic magnetic properties of materials. It is used for characterizing paramagnetic, ferromagnetic, ferrimagnetic and antiferromagnetic materials, spin glasses, conventional and high Tc superconductors.

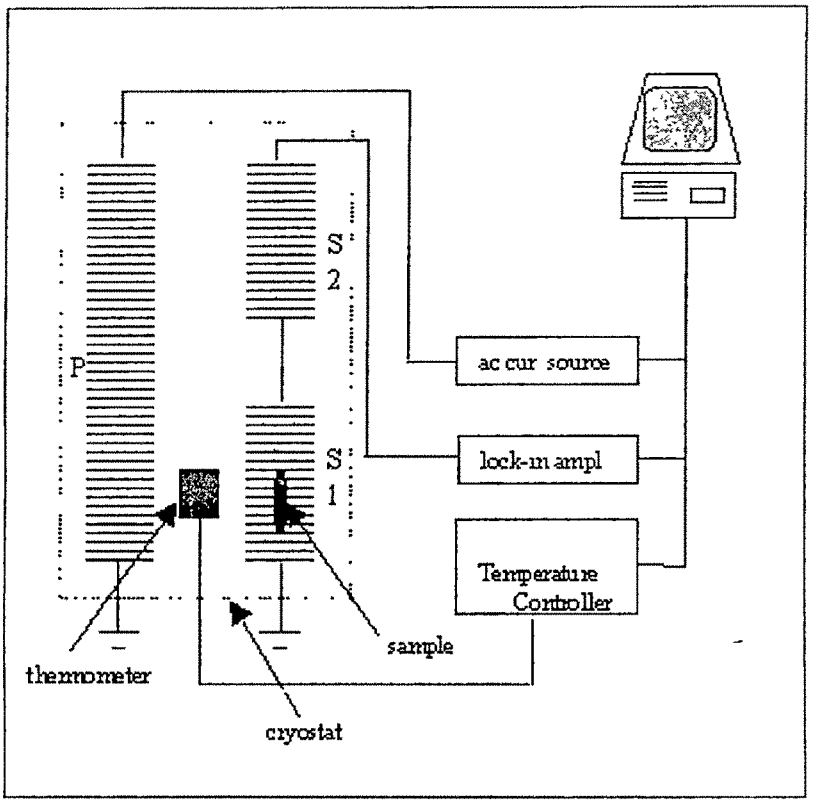

Fig 2.5

2.4.2 Basic principles:

In this technique, AC field is applied to a sample and the resulting AC moment is measured. Because the induced sample moment is time-dependent, AC measurements yield information about magnetization dynamics which are not obtained in DC measurements, where the sample moment is constant during the measurement time.

AC susceptometer mainly consists of primary coil and two secondary coils. Fig 2.5 above shows the block diagram of AC Suscpetometer setup. An AC current is passed through the coil which produces an AC magnetic field over a sample kept between primary and secondary coils. The two secondary coils in series are wound oppositively. Hence the variation in flux created by the sample is observed. The resultant signal is measured by a phase sensitive detector which produces an output voltage proportional to AC susceptibility of the sample. Through this measurements one can measure both the real or in phase component (χ^1) and imaginary or out of phase component (χ^{11}).

The temperature dependence of AC susceptibility can give idea of whether a magnetic sample contains Multidomain, single domain or super paramagnetic particles. The cusp at freezing temperature in the low field a.c. susceptibility versus temperature characterizes the spin glass behviour [10]. Furthermore, the location of the cusp is dependent on the frequency of the AC susceptibility measurement, a feature that is not present in other magnetic systems and therefore confirms the spin-glass phase.

AC susceptibility measurements is an important tool in the characterization of small ferromagnetic particles which exhibit superparamagnetism[11]. In this phenomena, the particles exhibit single-domain ferromagnetic behavior below the blocking temperature, *TB* , and are superparamagnetic above *TB* . In the superparamagnetic state, the moment of each particle freely rotates, so a collection

of particles acts like a paramagnet where the constituent moments are ferromagnetic particles (rather than atomic moments as in a normal paramagnet). So, when the thermal energy equals to the volume energy of a single domain particle it shows superparamagnetic nature and spontaneously fluctuate between their easy direction yields zero coericivity and as a result the peak is observed in low field a.c. susceptibility versus temperature curve [12]

2.5 Hall Effect

2.5.1 Introduction:

The Hall Effect describes the behavior of the free carriers in a semiconductor when the electric and magnetic field are applied. A particle with charge Q, velocity V and moving within a magnetic field B will experience the lorentz force $F = Q(v \times B)$. The force direction is mutually perpendicular to the directions of the particle velocity and magnetic field. When a conductor is placed in a magnetic field, the moving charges will experience a net force mutually perpendicular to the direction of current flow and the magnetic field. Under the influence of this force, the electrons will "pile up" on one edge of the conductor and positive charges will gather on the other edge. A lateral charge distribution results and gives rise to an electric field E which exerts a force F=QE opposite in direction to lorentz force. The relation between the voltage, current, and magnetic field can be generalized as follows:

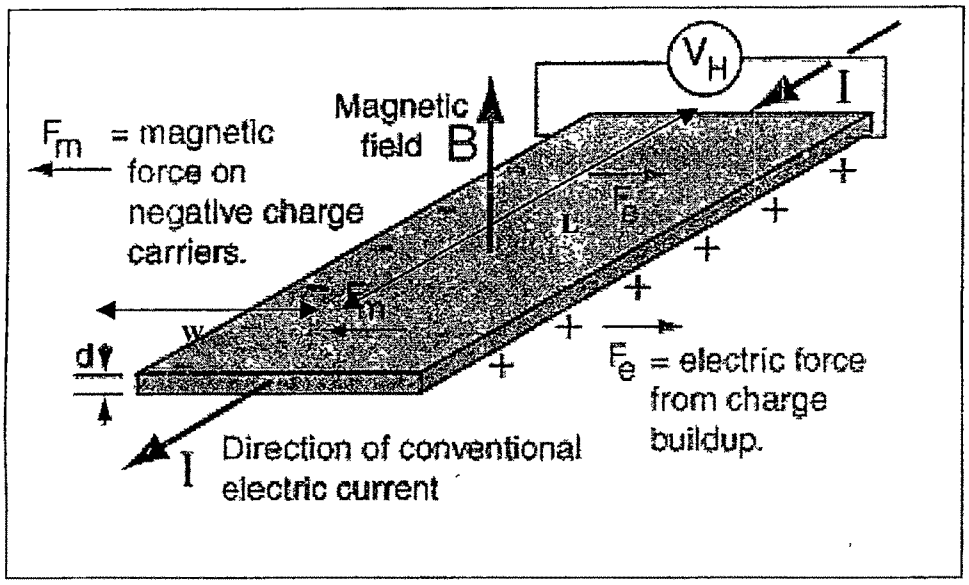

Fig 2.6

$$V_H = \frac{IB}{ned}$$

In previous page q was the notation for charge while here it is e. Use consistent notation

Where,

V_H = Hall voltage, I = Hall current, d = thickness of sample

B= magnetic field perpendicular to hall plate surface, n = Carrier concentration

2.5.2 Importance of Hall effect:

1. It can be used to determine the electronic structure of the substance i.e. whether these are metals, semiconductors or insulators.
2. The sign of the current carrying charge determines whether conduction is through electrons or holes.
3. Resistivity and Mobility of the charge carriers can be determined.

If T is the thickness , W is the width and L is the length of sample then knowing the resistance one can find out Resistivity as well as Mobility.

$$R = \frac{\rho L}{A}, \text{ so } \rho = \frac{RWd}{L} = \frac{V/I}{L/Wd}$$

Since the conductivity $\sigma = 1/\rho$ is equal to $q\mu_p p$, the mobility μ_p is just the ratio of the Hall coefficient and the resistivity. Measurements of the Hall coefficient and the resistivity over a range of temperatures yield plots of majority carrier concentration and mobility vs. temperature, a very useful data to have for semiconductors.

4. The carrier concentration of the charge carriers can be determined from Hall coefficient measured.

$$\text{i.e. } R_H = \frac{1}{ne}$$

Where, n is the carrier concentration and R_H = Hall coefficient.

2.5.3 Magnetoresistance: It is the measure of change in electrical conductivity associated with an applied electric field when a magnetic field is applied. The study of magnetic field effects on the transport properties of metals and semiconductors has been a well established and invaluable tool for the investigation of mobile carriers in crystals. Magnetoresistivity measurement determine the resistivity of materials in the presence of magnetic field. In metal with closed Fermi surface the magnetoresistivity does not saturate for any crystal orientation. The same occur for crystal of n-type and p-type semiconductor. In metal with equal no of electrons and holes such as Bi, Sb, and others the magnetoresitivity does not saturate for any crystal orientation and keeps on increasing as the magnetic field increases, same thing happens with for semiconductor with equal no of electron and holes.

References

1. G.K.Shenoy, F.E.Wagner and G.M.Kalvis, "Mossbauer Isomer Shifts", North Holland, Amsterdam, 1978
2. G.K.Werthiem, "Mossbauer Effect"Academic Press, London,1964
3. E.V.Meerwal, Com. Phys.Commun., 9 (1975) 117
4. A.J.F.Boyle and H.E.Hall, "Mossbauer effect", Rep. Progr. Phys. 25,441(1962)
5. N.N.Greenwood, and T.C.Gibbs, " Mossbauer Spectroscopy" ,Chapmann and Hall Ltd., London, (1971) 19
6. F.Frauenfelder and R.M.Steffen, "Alpha Beta and Gamma ray spectroscopy, Ed." K.Siegbahn, page 997, North Holland Publishing Company, (1965)
7. C.Gunther and I.Lindgreen, perturbed Angular Correlations, Eds. E.Karlsson, E.Mattheis and K.Seigbahn, North Holland Publishing Company, (1964)
8. R.M.Steffan abd K.Alder, " Electromagnetic interaction in Nuclear Spectroscopy", Ed W.D.Hamilton, North Holland, 1975
9. G.F.Knoll, " Radiation detection and Measurement", John willey, 1988
10. Murani A.P.J..Magn.Magn.Mater.5, 95 (1977)
11. L. Néel, C. R. Hebd. Seances Acad. Sci. 228, 664 (1949); Ann. Géophys. 5, 99 (1949). 5 W. F. Brown, Phys. Rev. 130, 1667 (1963)
12. Radhakrisnamurthy C, Likhite S.D., Deutch E.R. and Murthy G.S. Phys.Earth and planertary interiors, 26,37 (1981)
13. Peter Y. Yu, M.Cardona, Fundamentals of Semiconductors, Springer Veralg (1996).